Available online at www.sciencedirect.com
SCIENCE DIRECT®
International Journal of Heat and Mass Transfer 47 (2004) 3695–3705
International Journal of HEAT and MASS TRANSFER
www.elsevier.com/locate/ijhmt

Transient analysis of heat and mass transfer by natural convection over a vertical wavy surface

Jer-Huan Jang [a], Wei-Mon Yan [b,*]

[a] Department of Mechanical Engineering, Kuang-Wu Institute of Technology, Pei-To, Taipei 112, Taiwan
[b] Department of Mechatronic Engineering, Huafan University, Shih-Ting, Taipei 22305, Taiwan

Received 25 August 2003; received in revised form 29 March 2004
Available online 8 May 2004

Abstract

The transient behaviors of natural convection heat and mass transfer along a vertical wavy surface subjected to step changes of wall temperature and wall concentration have been investigated numerically by using a simple coordinate transformation to transform the complex wavy surface into a flat plate. An implicit marching finite-difference scheme is employed for the analysis. It is well know that the buoyancy ratio N and Schmidt number Sc are the parameters of importance for heat and mass transfer. The wavy geometry is also an important factor for this problem. Numerical results show that the flow field takes more time to reach steady condition for a high amplitude-wavelength ratio α, small buoyancy ratio N, and large Schmidt number Sc. The effects of wavy geometry, buoyancy ratio N and Schmidt number Sc on the transient local skin-friction, local Nusselt number and local Sherwood number have been discussed in detail.
© 2004 Elsevier Ltd. All rights reserved.

1. Introduction

The analysis of natural convection has been of considerable interest to engineers and scientists. Most studies of natural convection are mainly concerned with heat convection solely. However, Gebhart and Pera [1] indicated that buoyancy effects from concentration gradients can be as important as those from temperature gradients. There are applications of interest in which combined heat and mass transfer by natural convection, such as design of chemical processing equipment, design of heat exchangers, formation and dispersion of fog, distributions of temperature and moisture over agricultural fields, pollution of the environments and thermo-protection systems.

Extensive studies of natural convection of heat and mass transfer have been investigated in the past decades and various extensions of the problem have been reported in the literature. Yan and Lin [2] studied numerically on natural convection heat and mass transfer with film evaporation and condensation in vertical concentric annular ducts. They found that the heat transfer is enhanced due to heat exchange with phase changed. In addition, the enhancement of heat transfer due to mass transfer is more significant with a higher wetted wall temperature. Chang et al. [3] investigated the combined buoyancy effects of thermal and mass diffusion on the natural convection flows in a vertical open tube. They found that the heat transfer augmentation through mass diffusion connected with film evaporation is considerable.

Massive amount of works on heat and mass transfer have focused mainly on regular geometries, such as a vertical flat plate [4–9], flat plate with inclination [10–12], parallel-plate channel [13–16], and rectangular ducts [17–19], etc. However, it is necessary to study the heat and mass transfer for complex geometries because the prediction of heat and mass transfer for irregular surfaces is a topic of fundamental importance and irregular surfaces often appeared in many applications, for examples, flat-plate solar collectors and flat-plate condensers in refrigerators. Few studies have considered the effects of complex geometries. Wang and

* Corresponding author. Tel.: +886-2-2663-2102/2201; fax: +886-2-2663-2143.
E-mail address: wmyan@huafan.hfu.edu.tw (W.-M. Yan).

0017-9310/$ - see front matter © 2004 Elsevier Ltd. All rights reserved.
doi:10.1016/j.ijheatmasstransfer.2004.03.010

Nomenclature

a	amplitude of the wavy surface (m)
c	concentration
C	dimensionless concentration
C_f	skin-friction coefficient
C_p	specific heat of fluid at constant pressure ($kJ\,kg^{-1}\,K^{-1}$)
D	mass diffusivity ($m^2\,s^{-1}$)
g	gravitational acceleration ($m\,s^{-2}$)
k	conductivity ($W\,m^{-1}\,K^{-1}$)
L	wavelength of the wavy surface (m)
N	buoyancy ratio, Eq. (7)
Nu	Nusselt number
P	pressure ($N\,m^{-2}$)
Pr	Prandtl number
Sc	Schmidt number
Sh	Sherwood number
T	temperature (K)
t	time (s)
U, V	dimensionless velocity
$\widetilde{U}$	characteristic velocity
u, v	velocity components in the x and y directions, respectively ($m\,s^{-1}$)
X, Y	dimensionless coordinate system
x, y	coordinate system (m)

Greek symbols

α	amplitude-wavelength ratio, a/L
β_T	thermal expansion coefficient
β_c	concentration expansion coefficient
σ	dimensionless coordinate of the wavy surface
$\bar{\sigma}$	coordinate of the wavy surface, Eq. (1)
μ	viscosity ($kg\,m^{-1}\,s^{-1}$)
ρ	fluid density ($kg\,m^{-3}$)
θ	dimensionless temperature
τ	dimensionless time

Superscript

$*$	non-dimensional quantity

Subscripts

∞	conditions far away from the surface
c	caused by concentration
m	mean value
T	caused by temperature
w	surface condition
x	local value

Kleinstreuer [20] investigated the thermal convection on micropolar fluids passing a convex with suction/injection. Wu et al. [21] developed a numerical model to study the effectiveness of dehydration media for wedge-shaped surface with mass and heat transfer. Yih [22] studied the heat and mass transfer characteristic in natural convection flow over a truncated cone subjected to uniform wall temperature and concentration or uniform heat and mass flux embedded in porous media.

Yao [23–25] first investigated the natural convection heat transfer from an isothermal vertical wavy surface and used an extended Prantdl's transposition theorem and a finite-difference scheme. He proposed a simple transformation to study the natural convection heat transfer for an isothermal vertical sinusoidal surface. Chen and Wang [26,27] analyzed the transient forced and free thermal convection along a wavy surface in micropolar fluids. Chiu and Chou [28] investigated the natural convection heat transfer along a vertical wavy surface in micropolar fluids. Recently, the study of natural convection heat transfer along a wavy surface in a thermally stratified fluid saturated porous medium with the effects of wave phase was presented by Rathish Kumar and Shalini [29]. Besides, Rathish Kumar and his colleagues [30–33] performed a series of studies about the natural convection heat transfer in porous enclosures. Cheng [34,35] studied coupled heat and mass transfer by natural convection flow along a wavy conical surface and vertical wavy surface in a porous medium.

The above literatures survey shows that previous studies about vertical wavy surfaces mostly are concerned with micropolar fluids or porous media. In these studies, the governing equations or the boundary conditions for the analysis are much simpler. Recently, Jang et al. [36,37] has studied numerically on natural and mixed convection heat and mass transfer along a vertical wavy surface with Newtonian fluids.However, this study only pertains to steady flow. The transient natural heat and mass transfer along a vertical wavy surface, especially in Newtonian fluid, has not been well investigated. The objective of the present investigation is to analyze the transient natural convection heat and mass transfer in Newtonian fluid flow along a vertical wavy surface numerically by using Prandtl's transposition theorem. The numerical results, including the developments of friction factor, Nusselt number as well as Sherwood number along the wavy surface are presented. The effects of wavy geometry α, buoyancy ratio N and Schmidt number Sc on the transient local skin-friction, local Nusselt number and local Sherwood number have been examined in detail.

2. Analysis

2.1. Problem statement

The geometry of this problem as schematically shown in Fig. 1 is a vertical wavy surface. The u and v velocity are the velocity components in the x and y directions respectively. The flow is transient, laminar and incompressible with simultaneous heat and mass along a semi-infinite vertical wavy surface. The thermo-physical properties are assumed to be constant except the buoyancy term in the x momentum equation. The Boussinesq approximation is used to characterize the buoyancy effect.

The wavy surface of the plate is described in the function below:

$$y = \bar{\sigma}(x) = a \cdot \sin(2\pi x/L) \tag{1}$$

where the origin of the coordinate system is placed at the leading edge of the vertical surface. Initially, i.e. $t < 0$, the fluid oncoming to the surface is still quiescent and both the fluid and the wavy surface have constant temperature T_∞ and concentration c_∞. At time $t = 0$, the temperature and the concentration of the wavy surface are suddenly changed to new levels, T_w and c_w, respectively. Due to the temperature and concentration differences between the wavy surface and ambient, the combined buoyancy forces are then generated, which in turn, induce the fluid motion in the ambient.

2.2. Governing equations

With descriptions of the problem and the assumptions above, the governing equations which are those of conservation of mass, momentum, energy and concentration, may be written as:

$$\frac{\partial u}{\partial x} + \frac{\partial v}{\partial y} = 0 \tag{2}$$

$$\rho\left(\frac{\partial u}{\partial t} + u\frac{\partial u}{\partial x} + v\frac{\partial u}{\partial y}\right) = -\frac{\partial P}{\partial x} + \mu\left(\frac{\partial^2 u}{\partial x^2} + \frac{\partial^2 u}{\partial y^2}\right) + \rho g\beta_T(T - T_\infty) + \rho g\beta_c(c - c_\infty) \tag{3}$$

$$\rho\left(\frac{\partial v}{\partial t} + u\frac{\partial v}{\partial x} + v\frac{\partial v}{\partial y}\right) = -\frac{\partial P}{\partial y} + \mu\left(\frac{\partial^2 v}{\partial x^2} + \frac{\partial^2 v}{\partial y^2}\right) \tag{4}$$

$$\rho C_p\left(\frac{\partial T}{\partial t} + u\frac{\partial T}{\partial x} + v\frac{\partial T}{\partial y}\right) = k\left(\frac{\partial^2 T}{\partial x^2} + \frac{\partial^2 T}{\partial y^2}\right) \tag{5}$$

$$\frac{\partial c}{\partial t} + u\frac{\partial c}{\partial x} + v\frac{\partial c}{\partial y} = D\left(\frac{\partial^2 c}{\partial x^2} + \frac{\partial^2 c}{\partial y^2}\right) \tag{6}$$

Introduce the dimensionless parameters in the following,

$$\begin{aligned} &x^* = \frac{x}{L}; \qquad y^* = \frac{y - \bar{\sigma}}{L}Gr^{1/4}; \qquad u^* = \frac{\rho L}{\mu Gr^{1/2}}u; \\ &v^* = \frac{\rho L}{\mu Gr^{1/4}}(v - \sigma' u); \qquad P^* = \frac{\rho L^2}{\mu^2 Gr}P; \\ &Gr = \frac{g\beta_T(T_w - T_\infty)\rho^2 L^3}{\mu^2}; \qquad Pr = \frac{\mu C_p}{K}; \\ &Sc = \frac{\mu}{\rho D}; \qquad \theta = \frac{T - T_\infty}{T_w - T_\infty}; \qquad C = \frac{c - c_\infty}{c_w - c_\infty}; \\ &N = \frac{\beta_C(c_w - c_\infty)}{\beta_T(T_w - T_\infty)}; \qquad \sigma = \frac{\bar{\sigma}}{L}; \qquad \tau = \frac{\mu Gr^{1/2}t}{\rho L^2} \end{aligned} \tag{7}$$

and ignoring the small order terms in Gr, the governing equations then become

$$\frac{\partial u^*}{\partial x^*} + \frac{\partial v^*}{\partial y^*} = 0 \tag{8}$$

$$\frac{\partial u^*}{\partial \tau} + u^*\frac{\partial u^*}{\partial x^*} + v^*\frac{\partial u^*}{\partial y^*} = -\frac{\partial P^*}{\partial x^*} + \sigma'\frac{\partial P^*}{\partial y^*}Gr^{1/4} + \left(1 + \sigma'^2\right)\frac{\partial^2 u^*}{\partial y^{*2}} + \theta + NC \tag{9}$$

$$u^{*2}\sigma'' + \sigma'(\theta + NC) = \sigma'\frac{\partial P^*}{\partial x^*} - \left(1 + \sigma'^2\right)\frac{\partial P^*}{\partial y^*}Gr^{1/4} \tag{10}$$

$$\frac{\partial \theta}{\partial \tau} + u^*\frac{\partial \theta}{\partial x^*} + v^*\frac{\partial \theta}{\partial y^*} = \frac{1}{Pr}\left(1 + \sigma'^2\right)\frac{\partial^2 \theta}{\partial y^{*2}} \tag{11}$$

$$\frac{\partial C}{\partial \tau} + u^*\frac{\partial C}{\partial x^*} + v^*\frac{\partial C}{\partial y^*} = \frac{1}{Sc}\left(1 + \sigma'^2\right)\frac{\partial^2 C}{\partial y^{*2}} \tag{12}$$

It is noticeable that σ' and σ'' indicate the first and second differentiations of σ with respect to x^*, therefore, $\sigma' = \frac{d\bar{\sigma}}{dx} = \frac{d\sigma}{dx^*}$ and $\sigma'' = \frac{d\sigma'}{dx^*}$. For the current problem, the

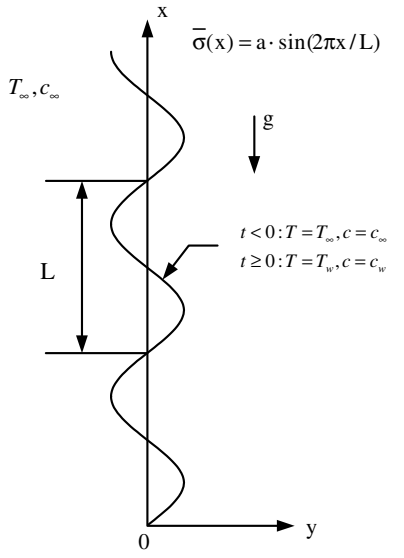

Fig. 1. Schematic diagram of the physical system.

pressure gradient $\frac{\partial P^*}{\partial x^*}$ is zero. Therefore, Eq. (9) can be reduced to the following equation after eliminating $\frac{\partial P^*}{\partial y^*}$ in Eqs. (9) and (10).

$$\frac{\partial u^*}{\partial \tau} + u^*\frac{\partial u^*}{\partial x^*} + v^*\frac{\partial u^*}{\partial y^*} = \frac{1}{1+\sigma'^2}(\theta + NC - u^{*2}\sigma'\sigma'') + (1+\sigma'^2)\frac{\partial^2 u^*}{\partial y^{*2}} \tag{13}$$

Use the following transformation in order to remove the singularity at the leading edge [17],

$$X = x^*; \qquad Y = \frac{y^*}{(4x^*)^{1/4}};$$
$$U = \frac{u^*}{(4x^*)^{1/2}}; \qquad V = (4x^*)^{1/4}v^* \tag{14}$$

Eqs. (8) and (11)–(13) in the parabolic coordinates (X, Y) then become

$$2U + 4X\frac{\partial U}{\partial X} - Y\frac{\partial U}{\partial Y} + \frac{\partial V}{\partial Y} = 0 \tag{15}$$

$$\frac{\partial U}{\partial \tau} + 4XU\frac{\partial U}{\partial X} + (V - UY)\frac{\partial U}{\partial Y} + \left(2 + \frac{4X\sigma'\sigma''}{1+\sigma'^2}\right)U^2 = \frac{1}{1+\sigma'^2}(\theta + NC) + (1+\sigma'^2)\frac{\partial^2 U}{\partial Y^2} \tag{16}$$

$$\frac{\partial \theta}{\partial \tau} + 4XU\frac{\partial \theta}{\partial X} + (V - UY)\frac{\partial \theta}{\partial Y} = \frac{1}{Pr}(1+\sigma'^2)\frac{\partial^2 \theta}{\partial Y^2} \tag{17}$$

$$\frac{\partial C}{\partial \tau} + 4XU\frac{\partial C}{\partial X} + (V - UY)\frac{\partial C}{\partial Y} = \frac{1}{Sc}(1+\sigma'^2)\frac{\partial^2 C}{\partial Y^2} \tag{18}$$

2.3. Initial and boundary conditions

As mentioned earlier, the fluid oncoming to the surface is still quiescent and both the fluid and the wavy surface have constant temperature and concentration. At time $t = 0$, the temperature and the concentration of the wavy surface are suddenly changed to new levels. The appropriate initial condition can be written as:

$$t < 0: \quad T = T_\infty, \qquad c = c_\infty, \qquad u = v = 0 \tag{19}$$

For $t \geqq 0$, the boundary conditions for the problem are:

$$\text{At the wavy surface,} \quad u = 0, \qquad v = 0,$$
$$T = T_w, \qquad c = c_w \tag{20}$$

Matching with the quiescent free stream,

$$u = 0, \qquad v = 0, \qquad T = T_\infty, \qquad c = c_\infty \tag{21}$$

Substituting dimensionless parameters into the Eqs. (19)–(21), the corresponding initial and boundary conditions are

$$\tau < 0; \qquad U = V = \theta = C = 0 \tag{22}$$

$$\tau \geqq 0; \qquad Y = 0; \qquad U = V = 0;$$
$$\theta = 1; \qquad C = 1 \tag{23}$$

$$Y \to \infty; \qquad U \to 0; \qquad \theta \to 0; \qquad C \to 0 \tag{24}$$

2.4. Governing parameters

It is customary to express heat and mass transfer characteristic in terms of the flux rate divided by the temperature or concentration difference causing transfer. These values are then expressed in dimensionless form to obtain the local Nusselt and Sherwood numbers, respectively. The local heat and mass transfer rates are large when the normal velocity approaches the surface; they are small when the convective stream moves away from the surface. The heat and mass transfer mechanism along a wavy surface is different from that along a flat surface, and is modified by the fluid motion normal to the surface.

The local Nusselt number and Sherwood number are defined respectively as:

$$Nu_x = \frac{hx}{k} = -\left(\frac{Gr}{4X}\right)^{1/4}(1+\sigma'^2)^{1/2}\left(\frac{\partial \theta}{\partial Y}\right)_{Y=0} \tag{25}$$

$$Sh_x = \frac{h_D x}{D} = -\left(\frac{Gr}{4X}\right)^{1/4}(1+\sigma'^2)^{1/2}\left(\frac{\partial C}{\partial Y}\right)_{Y=0} \tag{26}$$

The local skin-friction coefficient C_{fx} is defined by

$$C_{fx} = \frac{2\tau_w}{\rho \widetilde{U}^2} \tag{27}$$

where $\widetilde{U} = \frac{\mu Gr^{1/2}}{\rho L}$ is a characteristic velocity and the shearing stress on the wavy surface is

$$\tau_w = \left[\mu\left(\frac{\partial u}{\partial y} + \frac{\partial v}{\partial x}\right)\right]_{y=0} \tag{28}$$

Substituting Eq. (28) into Eq. (27) in terms of the non-dimensional quantities, we have

$$C_{fx} = \left(\frac{4X}{Gr}\right)^{1/4} 2(1-\sigma'^2)\left(\frac{\partial U}{\partial Y}\right)_{Y=0} \tag{29}$$

3. Numerical approach

Because of the non-linear interactions among the momentum equations, the energy equation and the concentration equation, solution for the problem can be solved by numerical finite-difference procedures. The governing equations are parabolic in X and τ. Hence the solution can be marched in time and the downstream direction. For the purpose of the numerical stability, a fully implicit formulation in time is adopted. The unsteady terms are approximated by backward differ-

ence. The axial convection is approximated by the upstream difference and the transverse convection and diffusion terms by the central difference is used to transform the governing equations into the finite-difference equations. The resulting system of algebraic equations can be cast into a tri-diagonal matrix equation, which can be efficiently solved by the Thomas algorithm [38]. During each transient and axial step, the numerical evaluation is iterated until the relative errors of the velocity, temperature and concentration at sequential iterations are less than 10^{-5}. If not, repeat the iterations for the current axial location. If yes, apply the above procedures from $X = 0$ to the desired downstream location ($X = 4.0$). Then march the solution from the onset of the transient to the final steady state. The steady-state criteria for the relative deviations of the variables, U, V, θ and C, between two time intervals are less than 10^{-4}. The detailed numerical procedures are similar to those of Ref. [39]. In the study, 251 non-uniform grid points were employed in the transverse direction (Y). Some of the calculations were tested using 501 grid points in the Y-direction, but no significant improvement over the 251 grid points was found. Additionally, there are 401 grid points in the marching direction. In the program test, a finer axial step size was tried and found to give acceptable accuracy. For the time interval, the first time interval is set to be 10^{-4}. The sequential time interval is then enlarged by 1%. To further check the adequacy of the numerical scheme used in this work, the results for the limiting case of natural convection heat transfer in a wavy surface were first obtained. Excellent agreement between the present predictions and those of Yao [23] was found. Besides, the predicted results of natural convection heat and mass transfer at steady state agree with the related work [36]. Through these program tests, it was found that the present numerical method is suitable for this study.

4. Results and discussion

In the present study, numerical calculations are performed for the wavy surface described by $\bar{\sigma}(x) = a \cdot \sin(2\pi x/L)$ or dimensionless $\sigma(X) = \alpha \cdot \sin(2\pi X)$. To simplify the analysis, the effects of wave phase of the

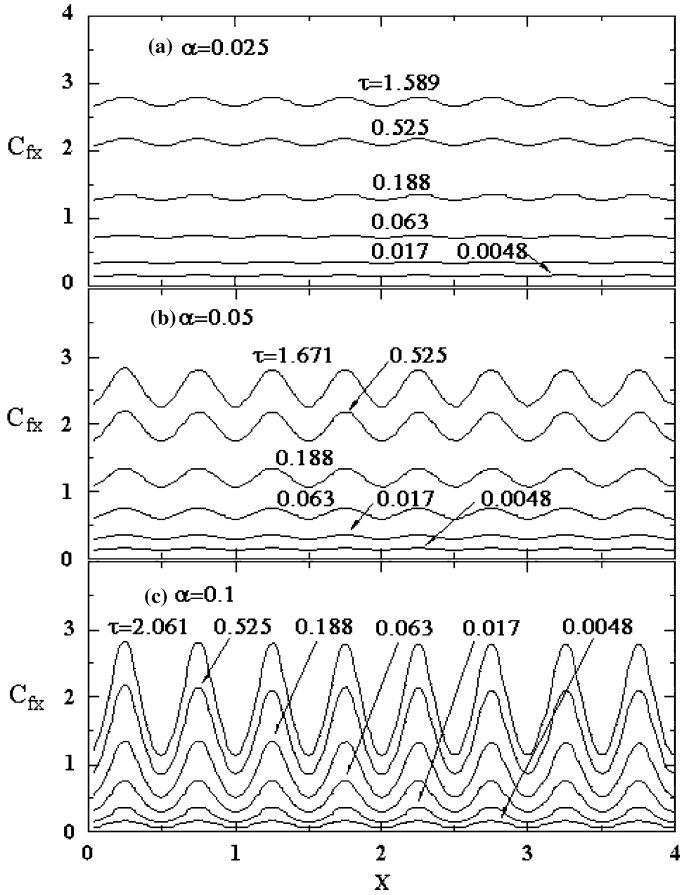

Fig. 2. Effects of amplitude-wavelength ratio α on the skin-friction coefficient at different time steps. (a) $\alpha = 0.025$, $N = 2$ and $Sc = 1.3$; (b) $\alpha = 0.05$, $N = 2$ and $Sc = 1.3$; (c) $\alpha = 0.1$, $N = 2$ and $Sc = 1.3$.

wavy plate are not considered in the present study. The wave phase may affect the natural convection heat and mass transfer. This will be examined in the near future. In fact, Rathish Kumar et al. [29–33] have presented some results about the effects of wave phase on heat transfer in different problems. In this work, three values of amplitude-wavelength ratio (i.e. $\alpha = 0.025$, 0.05, and 0.1) are used. The effect of governing physical parameters, such as amplitude-wavelength ratio α, buoyancy ratio N and Schmidt number Sc ranging from 0.6 to 2 are examined. The Prandtl number Pr is set equal to a fixed value of 0.7 throughout this investigation. The typical chosen values are taken as $\alpha = 0.05$, $N = 2$, and $Sc = 1.3$. Because the leading edge of the wavy surface is a singular point, the results near this particular position are not presented in these figures.

Fig. 2 shows the effects of wavy geometry on the transient local skin-friction along the X-axis. It is clearly seen that as α increases, the skin-friction fluctuates with greater amplitude for a given time step. But the maximum values of skin-friction remain the same. Initially the buoyancy-induced flow velocity is relatively low at the initial transient. Therefore, the hydrodynamic boundary layer thickness and the wall shear stress remain small. But, as the time proceeds, the hydrodynamic boundary layer thickness increases and the wall shear stress increases, which in turn, the skin-friction coefficient increases as well. It is obvious that the increase of skin-friction coefficient on the trough is less than those on the crest as time progresses. Therefore, the skin-friction coefficient fluctuates more with time. It is also noted that the fluctuation frequency of the skin-friction coefficient is half of that of the wavy surface for different time steps. The reason has been explained in Jang et al. [36]. Furthermore, it is observed that when the required non-dimensional time for reaching steady condition is 1.589, 1.671 and 2.061 for $\alpha = 0.025$, 0.05, and 0.1, respectively. This result indicates that the flow field of a higher amplitude-wavelength ratio needs more time to reach the steady condition.

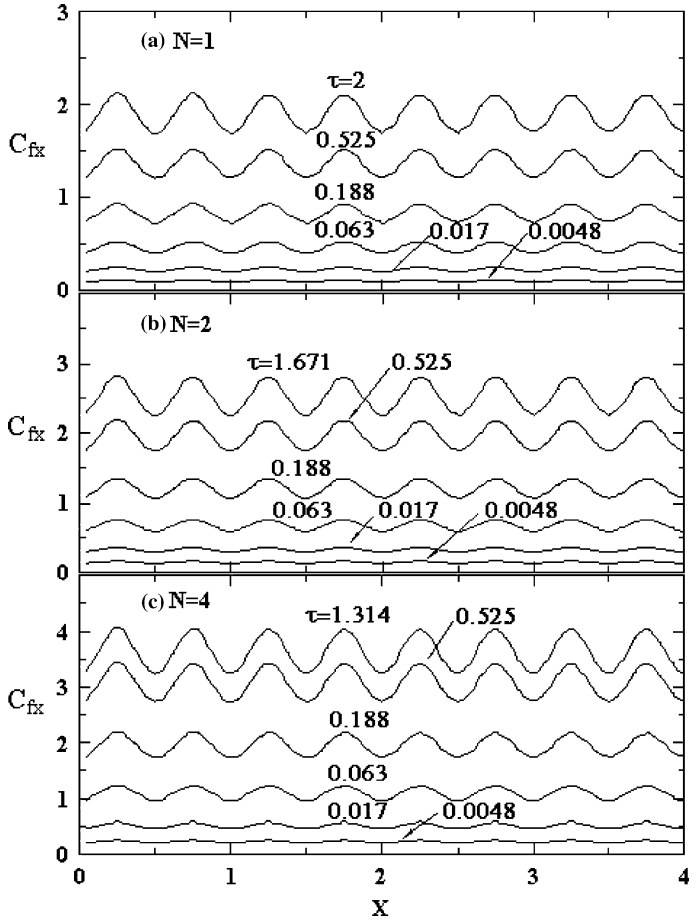

Fig. 3. Effects of buoyancy ratio N on the skin-friction coefficient at different time steps. (a) $N = 1$, $\alpha = 0.05$ and $Sc = 1.3$; (b) $N = 2$, $\alpha = 0.05$ and $Sc = 1.3$; (c) $N = 4$, $\alpha = 0.05$ and $Sc = 1.3$.

Fig. 3 represents the buoyancy ratio effect on transient local skin-friction along the X-axis. It is noted that the local skin-friction coefficient has similar distribution for different values of N and increases as N increases for a given time. This is due to the fact that the buoyancy force from species diffusion assists the thermal buoyancy force. Therefore, a higher skin-friction coefficient can be obtained for a higher value of N. It is interesting to see that the non-dimensional time required to reach steady condition is 2, 1.67, and 1.314 for $N = 1$, 2, and 4, respectively. In other words, a higher buoyancy ratio would shorten the time required to reach steady condition. This trend is also found in the results of Jang et al. [40].

In order to study the influence of Schmidt number on transient local skin-friction, the distributions of skin-friction along the X-axis with various Sc are shown in Fig. 4. It is found that the skin-friction coefficient has similar profiles and decreases with the increase in Sc for a given location and time step. According to the definition of Sc, the ratio of dynamic viscosity to diffusivity, an increase of Sc represents to increase the hydrodynamic boundary layer thickness with a fixed diffusivity, and this will cause the skin-friction coefficient to decreases. It is also shown that the non-dimensional times required for reaching steady condition are 1.638, 1.671, and 1.774 for $Sc = 0.6$, 1.3, and 2.0, respectively. This result indicates that the non-dimensional time required for reaching steady condition increases as Sc increases.

The heat and mass transfer varies along the wavy surface at the transient, but the fluctuations are relatively small when plotting figure at the transient. Therefore, only a fixed axial position is chosen to show the transient heat and mass transfer along the wavy surface. The effects of α, N and Sc on Nusselt and Sherwood numbers at $X = 1.0$ as a function of time are presented in Figs. 5 and 6, respectively. The Nusselt and Sherwood numbers are nearly the same during the initial transient regime. This is because the heat and mass transfer processes are dominated by pure heat conduction and pure mass diffusion during the initial transient

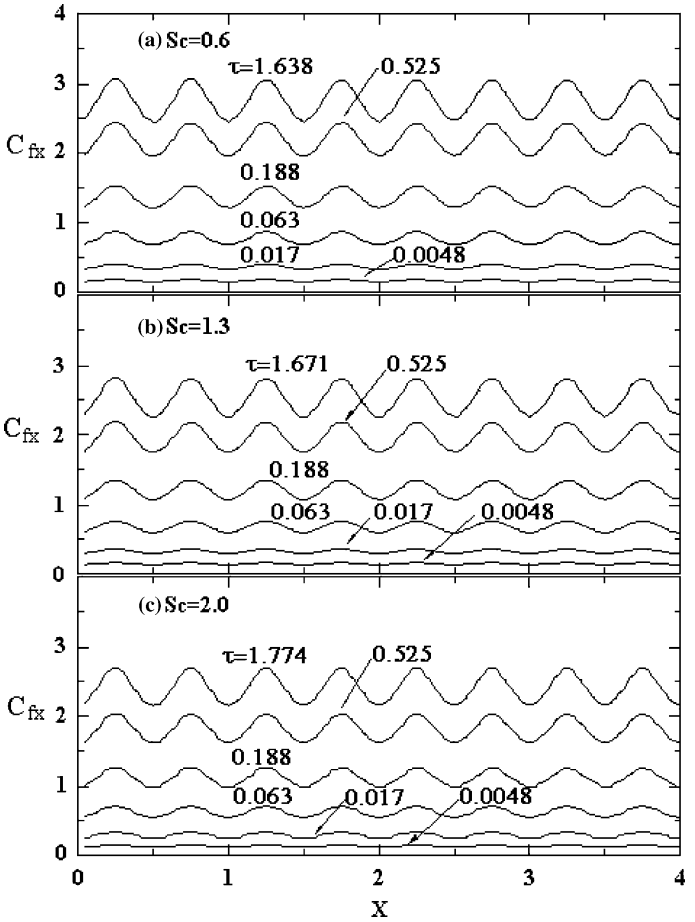

Fig. 4. Effects of Schmidt number Sc on the skin-friction coefficient at different time steps. (a) $Sc = 0.6$, $\alpha = 0.05$ and $N = 2$; (b) $Sc = 1.3$, $\alpha = 0.05$ and $N = 2$; (c) $Sc = 2.0$, $\alpha = 0.05$ and $N = 2$.

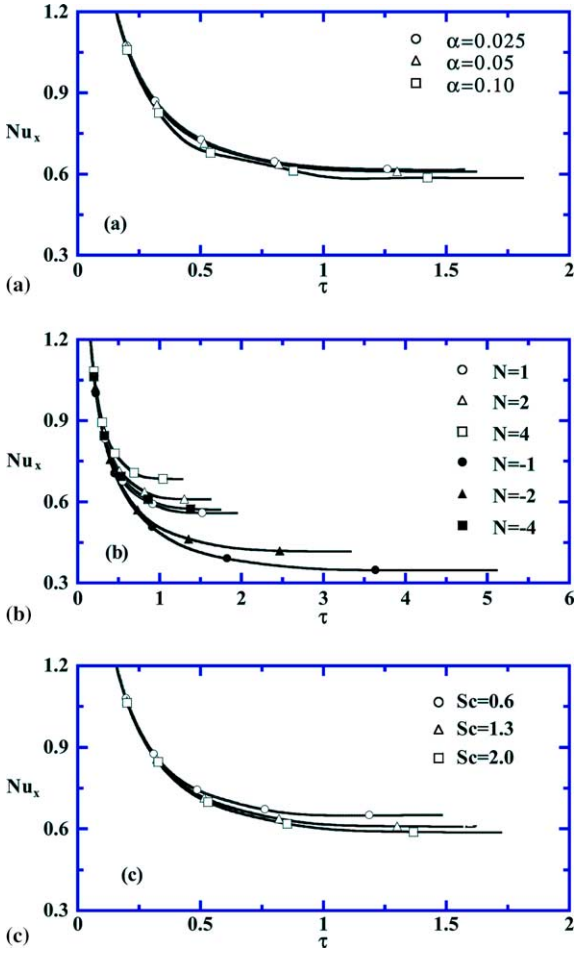

Fig. 5. Effects of different parameters on unsteady distributions of Nusselt number at $X = 1.0$. (a) $N = 2$ and $Sc = 1.3$; (b) $\alpha = 0.05$ and $Sc = 1.3$; (c) $\alpha = 0.05$ and $N = 2$.

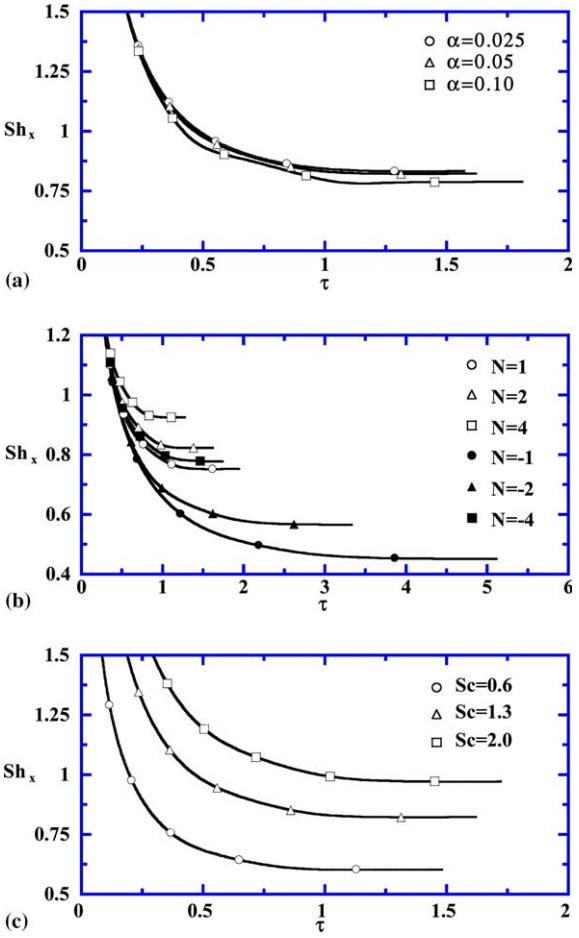

Fig. 6. Effects of different parameters on unsteady distributions of Sherwood number at $X = 1.0$. (a) $N = 2$ and $Sc = 1.3$; (b) $\alpha = 0.05$ and $Sc = 1.3$; (c) $\alpha = 0.05$ and $N = 2$.

regime. It is also observed that both the local Nusselt and Sherwood numbers decrease uniformly with time. During the initial period following the step changes in the wall temperature and wall concentration, the thermal and concentration boundary layers are extremely small. Thus, the gradients of temperature and concentration distribution on the surface are large. Therefore, the values of Nusselt and Sherwood numbers are large which represents a higher rate of heat and mass transfer. As time increases, the free convection effect becomes more pronounced and the thermal and concentration boundary layer thicknesses increase. Therefore, the local Nusselt and Sherwood numbers decrease, reducing the heat and mass transfer rates.

In Figs. 5(a) and 6(a), it is noted that the *Nu* and *Sh* are not much affected for smaller geometry factor. However, the *Nu* and *Sh* do decrease as α increases. The effect of buoyancy ratio on heat and mass transfer are shown in Figs. 5(b) and 6(b). The negative N represents an opposing buoyancy flow. It is found that the *Nu* and *Sh* increase as the absolute value of N increases. This is the reason of larger buoyancy force caused by the concentration difference. It is also noted that the *Nu* and *Sh* of opposing flow are always less than that of imposing flow. This could be realized that the convection velocity of opposing flow is always smaller than that of imposing flow causing the decrease in heat and mass transfer.

Effect of Schmidt number on the transient local Nusselt number is plotted in Fig. 5(c). It is shown that as *Sc* increases, *Nu* decreases. This is due to the fact that a larger *Sc* number is associated with a thinner concentration boundary relative to the thermal boundary layer thickness for *Pr* as a constant. Consequently, buoyancy effects due to mass transfer are diminished in the thermal boundary layer, and hence the influence of buoyancy ratio on heat transfer diminished with increasing *Sc*. In

Fig. 6(c), it can be clearly seen that *Sh* increases as *Sc* increases. This trend is analogous to heat transfer in that the heat transfer rate is increased as *Pr* increases. The reason for this is that a larger *Sc* corresponding to a thinner concentration boundary layer and this will cause the concentration gradient on the wall increase, therefore by the definition of *Sh*, *Sh* increases. That is the mass transfer rate increases with increasing *Sc*.

In order to understand the influence of velocity, temperature and concentration on the transient free convection, the dimensionless axial velocity, temperature and concentration at $X = 4.0$ along Y-axis as a function of time are illustrated in Fig. 7. It is seen that the axial velocity increases with time and the hydrodynamic, thermal and concentration boundary layers increase as well. It is noted that the temperature and concentration distributions display much similarity and the thermal boundary layer is thicker than the concentration boundary layer. In the observation of Fig. 7, the hydrodynamic boundary layer is smaller than thermal boundary layer but larger than concentration boundary layer. It is shown that the gradients of temperature and concentration are decreasing while the gradient of velocity is increasing, which matches the inferences in previous description.

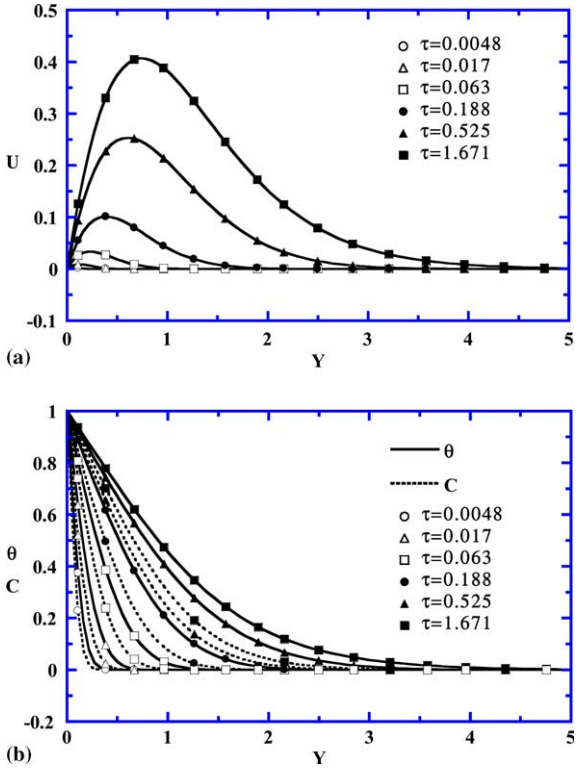

Fig. 7. Transient dimensionless axial velocity, temperature and concentration distributions at $X = 4.0$ for $\alpha = 0.05$, $N = 2$ and $Sc = 1.3$. (a) Axial velocity distributions; (b) temperature and concentration distributions.

5. Conclusions

The transient problem of natural convection heat and mass transfer along a wavy surface has been analyzed. The effects of amplitude-wavelength ratio α, buoyancy ratio N, and Schmidt number *Sc* on momentum, heat and mass transfer have been studied in detail. Brief summaries of the major results are listed in the following:

1. The flow field takes more time to reach steady condition for a higher amplitude-wavelength ratio α, small buoyancy ratio N, and large Schmidt number.
2. The fluctuation of local skin-friction coefficient C_{fx} increases with the amplitude-wavelength ratio α.
3. During the initial period, the thermal and concentration boundary layers are extremely small, the heat and mass transfer processes are dominated by pure heat conduction and pure mass diffusion. The Nusselt and Sherwood numbers are large at the initial transient.
4. The local Nusselt number Nu_x and Sherwood number Sh_x decrease as the time proceeds. While the local skin-friction coefficient C_{fx} increases as the time increases.
5. The local skin-friction coefficient, Nusselt number, and Sherwood number are enhanced as the buoyancy ratio N increases. This implies that the heat and mass transfer rates increase with the combined buoyancy forces due to species diffusion assisting the thermal buoyancy force.
6. Increasing Schmidt number *Sc* decreases the skin-friction coefficient and the local Nusselt number, but increases the local Sherwood number. In other words, the heat transfer rate is reduced while the mass transfer rate is enhanced as the Schmidt number is raised.

Acknowledgements

The authors would like to acknowledge the financial support of this work by the National Science Council, ROC through the contract NSC92-2212-E-211-001. The financial support from Kuang-Wu Institute of Technology through project KW-91-ME-008 is also acknowledged.

References

[1] B. Gebhart, L. Pera, The nature of vertical natural convection flows resulting from the combined buoyancy

effects of thermal and mass diffusion, Int. J. Heat Mass Transfer 14 (1971) 2025–2050.
[2] W.M. Yan, D. Lin, Natural convection heat and mass transfer in vertical annuli with film evaporation and condensation, Int. J. Heat Mass Transfer 44 (2001) 1143–1151.
[3] C.J. Chang, T.F. Lin, W.M. Yan, Natural convection flows in a vertical open tube resulting from combined buoyancy effects of thermal and mass diffusion, Int. J. Heat Mass Transfer 29 (1986) 1543–1552.
[4] E.V. Somers, Theoretical considerations of combined thermal and mass transfer from a flat plate, ASME J. Appl. Mech. 23 (1956) 295–301.
[5] W.G. Mather, A.J. Madden, E.L. Piret, Simultaneous heat and mass transfer in free convection, Ind. Eng. Chem. 49 (1957) 961–968.
[6] W.N. Gill, E.D. Casal, D.W. Zeh, Binary diffusion and heat transfer in laminar free convection boundary layers on a vertical plate, Int. J. Heat Mass Transfer 8 (1965) 1135–1151.
[7] F.A. Bottemanne, Theoretical solution of simultaneous heat and mass transfer by free convection about a vertical flat plate, Appl. Sci. Res. 25 (1971) 137–149.
[8] G.D. Callahan, W.J. Marner, Transient free convection with mass transfer on an isothermal vertical flat plate, Int. J. Heat Mass Transfer 19 (1976) 165–174.
[9] D. Angirasa, G.P. Peterson, I. Pop, Combined heat and mass transfer by natural convection with opposing buoyancy effects in a fluid saturated porous medium, Int. J. Heat Mass Transfer 40 (1997) 2755–2773.
[10] T.S. Chen, C.F. Yuh, Combined heat and mass transfer in natural convection on inclined surfaces, Numer. Heat Transfer 2 (1979) 233–250.
[11] L. Pera, B. Gebhart, Nature convection flows adjacent to horizontal surfaces resulting from the combined buoyancy effects of thermal and mass diffusion, Int. J. Heat Mass Transfer 15 (1972) 269–278.
[12] J.Y. Jang, W.J. Chang, Buoyancy-induced inclined boundary layer flow in a saturated porous medium resulting from combined heat and mass buoyancy effects, Int. Commun. Heat Mass Transfer 15 (1988) 17–30.
[13] W.M. Yan, Y.L. Tsay, T.F. Lin, Simultaneous heat and mass transfer in laminar mixed convection flows between vertical parallel plates with asymmetric heating, Int. J. Heat Fluid Flow 10 (1989) 262–269.
[14] W.M. Yan, T.F. Lin, Combined heat and mass transfer in natural convection between vertical parallel plates with film evaporation, Int. J. Heat Mass Transfer 33 (1989) 529–541.
[15] D.J. Nelson, B.D. Wood, Combined heat and mass transfer natural convection between vertical parallel plates, Int. J. Heat Mass Transfer 32 (1989) 1779–1787.
[16] D.J. Nelson, B.D. Wood, Combined heat and mass transfer natural convection between vertical parallel plates with uniform flux boundary conditions, Heat Mass Transfer 4 (1986) 1587–1592.
[17] K.Z. Lee, H.L. Tsai, W.M. Yan, Mixed convection heat and mass transfer in parallel rectangular ducts, Int. J. Heat Mass Transfer 40 (1997) 1621–1631.
[18] F.P. Incropera, J.A. Schutt, Numerical simulation of laminar mixed convection in the entrance region of horizontal rectangular ducts, Numer. Heat Transfer 8 (1985) 707–729.
[19] K. Ramakrishna, S.G. Rubin, P.K. Khosla, Laminar natural convection along vertical square ducts, Numer. Heat Transfer 5 (1982) 59–79.
[20] T.Y. Wang, C. Kleinstreuer, Thermal convection on micropolar fluids past two-dimensional or axisymmetric bodies with suction/injection, Int. J. Eng. Sci. 26 (1988) 1267–1277.
[21] C.H. Wu, D.C. Davis, J.N. Chung, L.C. Chow, Simulation of wedge-shaped product dehydration using mixtures of superheated steam and air in laminar flow, Numer. Heat Transfer 11 (1987) 109–123.
[22] K.A. Yih, Uniform transpiration effect on combined heat and mass transfer by natural convection over a cone in saturated porous media: uniform wall temperature/concentration or heat/mass flux, Int. J. Heat Mass Transfer 42 (1999) 3533–3537.
[23] L.S. Yao, Natural convection along a wavy surface, ASME J. Heat Transfer 105 (1983) 465–468.
[24] L.S. Yao, A note on Prandtl's transposition theorem, ASME J. Heat Transfer 110 (1988) 503–507.
[25] S.G. Moulic, L.S. Yao, Mixed convection along a wavy surface, ASME J. Heat Transfer 111 (1989) 974–979.
[26] C.K. Chen, C.C. Wang, Transient analysis of force convection along a wavy surface in micropolar fluids, AIAA J. Thermophys. Heat Transfer 14 (2000) 340–347.
[27] C.C. Wang, C.K. Chen, Transient force and free convection along a vertical wavy surface in micropolar fluids, Int. J. Heat Mass Transfer 44 (2001) 3241–3251.
[28] C.P. Chiu, H.M. Chou, Transient analysis of natural convection along a vertical wavy surface in micropolar fluids, Int. J . Eng. Sci. 32 (1994) 19–33.
[29] B.V. Rathish Kumar, Shalini, Non-Darcy free convection induced by a vertical wavy surface in a thermally stratified porous medium, Int. J. Heat Mass Transfer 47 (2004) 2353–2363.
[30] B.V. Rathish Kumar, P. Singh, P.V.S.N. Murthy, Effect of surface undulations on natural convection in a porous square cavity, ASME J. Heat Transfer 119 (1997) 848–851.
[31] P.V.S.N. Murthy, B.V. Rathish Kumar, P. Singh, Natural convection heat transfer from a horizontal wavy surface in a porous enclosure, Numer. Heat Transfer, Part A 31 (1997) 207–221.
[32] B.V. Rathish Kumar, P.V.S.N. Murthy, P. Singh, Free convection heat transfer from an isothermal wavy surface in a porous enclosure, Int. J. Numer. Methods Fluids 28 (1998) 633–661.
[33] B.V. Rathish Kumar, Shalini, Free convection in a non-Darcian wavy porous enclosure, Int. J. Eng. Sci. 41 (2003) 1827–1848.
[34] C.Y. Cheng, Natural convection heat and Mass transfer near a wavy cone with constant wall temperature and concentration in a porous medium, Mech. Res. Commun. 27 (2000) 613–620.
[35] C.Y. Cheng, Natural convection heat and mass transfer near a vertical wavy surface with constant wall temperature and concentration in a porous medium, Int. Commun. Heat Mass Transfer 27 (2000) 1143–1154.

[36] J.H. Jang, W.M. Yan, H.T. Liu, Natural convection heat and mass transfer along a vertical wavy surface, Int. J. Heat Mass Transfer 46 (2003) 1075–1083.
[37] J.H. Jang, W.M. Yan, Mixed convection heat and mass transfer along a vertical wavy surface, Int. J. Heat Mass Transfer 47 (2004) 419–428.
[38] C.V. Patankar, Numerical Heat Transfer Fluid Flow, Hemisphere/McGraw-Hill, New York, 1980.
[39] T.F. Lin, C.P. Yin, W.M. Yan, Transient laminar mixed convection heat transfer in vertical flat duct, ASME J. Heat Transfer 113 (1991) 384–390.
[40] J.Y. Jang, D.J. Tseng, H.J. Shaw, Transient free convection with mass transfer on a vertical plate embedded in a high-porosity medium, Numer. Heat Transfer, Part A 20 (1991) 1–18.